**MICROBIAL GENETICS, GENOMICS AND MOLECULAR BIOLOGY**

# Non-Mitochondrial Aconitase-2 Mediates the Transcription of Nuclear-Encoded Electron Transport Chain Genes in Fission Yeast

Ho-Jung Kim[1] · Soo-Yeon Cho[1] · Soo-Jin Jung[3,4] · Yong-Jun Cho[2] · Jung-Hye Roe[3] · Kyoung-Dong Kim[1]

## Abstract

Aconitase-2 (Aco2) is present in the mitochondria, cytosol, and nucleus of fission yeast. To explore its function beyond the well-known role in the mitochondrial tricarboxylic acid (TCA) cycle, we conducted genome-wide profiling using the *aco2ΔNLS* mutant, which lacks a nuclear localization signal (NLS). The RNA sequencing (RNA-seq) data showed a general downregulation of electron transport chain (ETC) genes in the *aco2ΔNLS* mutant, except for those in the complex II, leading to a growth defect in respiratory-prone media. Complementation analysis with non-catalytic Aco2 [*aco2ΔNLS + aco2(3CS)*], where three cysteines were substituted with serine, restored normal growth and typical ETC gene expression. This suggests that Aco2's catalytic activity is not essential for its role in ETC gene regulation. Our mRNA decay assay indicated that the decrease in ETC gene expression was due to transcriptional regulation rather than changes in mRNA stability. Additionally, we investigated the Php complex's role in ETC gene regulation and found that ETC genes, except those within complex II, were downregulated in *php3Δ* and *php5Δ* strains, similar to the *aco2ΔNLS* mutant. These findings highlight a novel role for nuclear aconitase in ETC gene regulation and suggest a potential connection between the Php complex and Aco2.

**Keywords** Aconitase · Electron transport chain (ETC) · Php complex · Respiration · Fission yeast

## Introduction

Aconitase is a well-known multifunctional protein (Boukouris et al., 2016; Castello et al., 2015; Jeffery, 2015, 2020). In higher eukaryotes, while mitochondrial aconitase acts as a mitochondrial tricarboxylic acid (TCA) cycle enzyme (Beinert et al., 1996), cytosolic aconitase acts as an RNA-binding protein, the so-called iron-regulatory protein (IRP) (Gourley et al., 2003; Gray et al., 1996; Klausner & Rouault,

1993; Lind et al., 2006; Lushchak et al., 2014; Rouault, 2006). Under iron-depleted condition, cytosolic aconitase loses its Fe-S cluster and changes its conformation to IRP (Dupuy et al., 2006). IRP binds to RNA stem-loop structures containing the iron-responsive element (IRE) and manipulates the stability of mRNA involved in iron metabolism (Muckenthaler et al., 2008; Piccinelli & Samuelsson, 2007; Volz, 2008). Furthermore, the role of aconitase as an IRP is observed in numerous microbial organisms, including *Escherichia coli*, *Bacillus subtilis*, and *Mycobacterium tuberculosis* (Alén & Sonenshein, 1999; Banerjee et al., 2007; Benjamin & Masse, 2014).

In the fission yeast *Schizosaccharomyces pombe*, two aconitases are Aco1 and Aco2. While Aco1 is directed to the mitochondria via a mitochondrial targeting sequence (MTS), Aco2 is a dual-targeting protein found within the mitochondria and in the nucleus and cytosol (Jung et al., 2015). Aco2 consists of an N-terminal aconitase domain with MTS and a C-terminal mitochondrial ribosomal domain (bL21) with a nuclear localization signal (NLS) (Fig. 1A) (Jung et al., 2015). Previous studies showed that Aco2 is required for mitochondrial translation (Jung et al., 2015) and heterochromatin maintenance in the nucleus

Ho-Jung Kim and Soo-Yeon Cho contributed equally to this work.

✉ Kyoung-Dong Kim
  kdkim0122@cau.ac.kr

1   Department of Systems Biotechnology, Chung-Ang
    University, Anseong 17546, Republic of Korea

2   Department of Molecular Bioscience, College of Biomedical
    Science, Kangwon National University, Chuncheon 24341,
    Republic of Korea

3   School of Biological Sciences, Seoul National University,
    Seoul 08826, Republic of Korea

4   Center for RNA Research, Institute for Basic Science,
    Seoul 08826, Republic of Korea

along with the heterochromatin protein Chp1 (Jung et al., 2019). We recently conducted an RNA-seq analysis using the NLS-deleted *aco2* (*aco2ΔNLS*) mutant to determine the role of Aco2 in the nucleus. Interestingly, we found that iron-transporter genes were upregulated in the mutant (Cho et al., 2021). Previously, we focused on exploring the reasons for the upregulation of iron-uptake genes in *aco2ΔNLS* mutants. By employing an mRNA decay assay, we verified the postponement of mRNA degradation related to iron transporters, resulting in an accumulation of these mRNAs in the *aco2ΔNLS* mutant. UV crosslinking RNA-IP (CLIP) assay showed that non-mitochondrial Aco2 is directly bound to iron-uptake mRNAs such as *fip1* and *str1* (Cho et al., 2021).

In this present study, we noticed that mitochondrial electron transport chain (ETC) genes were specifically downregulated in the mutant, and the decrease in the expression of ETC genes was not controlled by the post-transcriptional regulation of Aco2, unlike how Aco2 regulates iron-uptake genes. Here, we aimed to uncover the reason behind the reduced expression of nuclear-encoded ETC genes in the *aco2ΔNLS* mutant.

## Materials and Methods

### Yeast Strains and Culture Conditions

The fission yeast strains used in this study are listed in Table S1. The yeast strains were cultured in Edinburgh Minimal Medium (EMM) media at 32 °C (Forsburg & Rhind, 2006). For auxotrophic strains, required supplements (e.g., adenine, leucine, or uracil) were added to the media with the final concentration of 250 mg/L.

### Spotting Assay

For the spotting assay, *S. pombe* cells in mid-log phase were serially diluted tenfold and then spotted onto YE plates (YE, 0.5% yeast extract). These plates were supplemented with 3% glucose for fermentative growth or with 0.1% glucose, 3% galactose + 0.1% glucose, and 6% glycerol + 0.1% glucose for respiratory growth. The plates were incubated at 32℃ for 4 days. To create anaerobic conditions, AnaeroGen Compact (AN0020D; Oxoid) were inserted into W-Zip Seal Pouches (AG0060; Oxoid) containing the plates.

### Total RNA Isolation and Quantitative Reverse-Transcription-Polymerase Chain Reaction (qRT-PCR)

Total RNA was extracted from the exponentially growing cells cultured in EMM media using the RNeasy Mini Kit (74,104; Qiagen). Purified RNA was then treated with a

TURBO DNA-free Kit (AM1907; Thermo Fisher Scientific) according to the manufacturer's instructions to prevent the contamination of genomic DNA. For the cDNA synthesis, random hexamers (100 μM), RevertAid reverse transcriptase (EP0442; Thermo Fisher Scientific), and RiboLock RNase Inhibitor (EO0382; Thermo Fisher Scientific) were used as per the manufacturer's instructions. The qRT-PCR primers used in this study are shown in Table S2.

### RNA Sequencing (RNA-seq) and Data Analysis

The mRNA isolation and the sequencing library preparation were conducted using the NEBNext Ultra II RNA Library Prep Kit for Illumina (E7770S; New England Biolabs) and NEBNext Multiplex Oligos for Illumina (Index Primer Set 1) (E7335S; New England Biolabs) according to manufacturer's instructions. Sequencing was performed using an Illumina NovaSeq 6000 system (Macrogen).

Sequencing adapter removal and quality-based trimming were executed by Trimmomatic v0.36 for the raw data (Bolger et al., 2014). The processed reads were subsequently aligned to the reference genome (GCF_000002945.1) using hisat2 v2.2.1 with the '-k 1' parameter (Kim et al., 2019). The featureCounts was employed to quantify the reads aligned to individual coding sequences (CDS) (Liao et al., 2014). Finally, the read counts associated with each CDS were normalized using the DeSeq2 package (Love et al., 2014).

### Western Blot

Total protein extract was prepared as previously described (Kim et al., 2020). Proteins were electrophoresed on 10% SDS-PAGE gel and transferred to a nitrocellulose membrane (1,060,004; Cytiva). The membranes were incubated with 5% skim milk in TBST, overnight at 4 °C and then with primary antibody [1:10,000 dilution of α-DDDDK (M185-3L; MBL)] for 1 h at room temperature. This was followed by incubation with HRP-conjugated secondary antibody [1:20,000 dilution of α-mouse (1,706,516, Bio-Rad)] for 30 min.

### mRNA Decay Assay

The mRNA decay assay was performed as previously described (Cho et al., 2021). In brief, exponentially growing cells were treated with 1, 10-phenanthroline (300 μg/ml). The cells were harvested at the indicated time points and immediately mixed with an equal volume of ice-cold methanol to fix the cells. Total RNA was extracted from the cells, and cDNA was synthesized using oligo dT primers. The amount of RNA at each time point was quantified using qRT-PCR.

## Chromatin Immunoprecipitation (ChIP) Assay

ChIP analysis was performed as described previously, with some modifications (Kim et al., 2020). ChIP-seq against FLAG-tag was performed with OD600 of 1.0 cells and fixed with 3% formaldehyde. FLAG-tagged proteins were purified using Dynabeads Protein G (10004D; Invitrogen) and α-DDDDK antibody (M185-3L; MBL) at 4 °C. After elution, the DNA was purified with QIAquick PCR Purification Kit (28,106; Qiagen). The amount of precipitated DNA was quantified using qRT-PCR. The qRT-PCR primers used in this study are shown in Supplementary data (Table S2).

## Statistical Analysis

Data are presented as the mean ± SEM of more than three independent experiments. Statistical significance ($p$-value) was determined by Student's t-test (***$p < 0.001$; **$p < 0.01$; *$p < 0.05$; ns $p > 0.05$).

## Results

### Downregulation of Genes Related to Cellular Respiration in the *aco2ΔNLS* Mutant

To comprehensively investigate the role of nuclear Aco2, we performed transcriptome analysis using RNA-seq with both the *aco2ΔNLS* mutant and wild-type strains cultured in EMM media. The RNA-seq results revealed that 63 protein-coding genes were upregulated, while 161 were downregulated in the *aco2ΔNLS* mutant compared to the wild-type ($\log_2$FC < − 0.5). We used the online tool GOtermFinder (https://go.princeton.edu/cgi-bin/GOTermFinder) to analyze
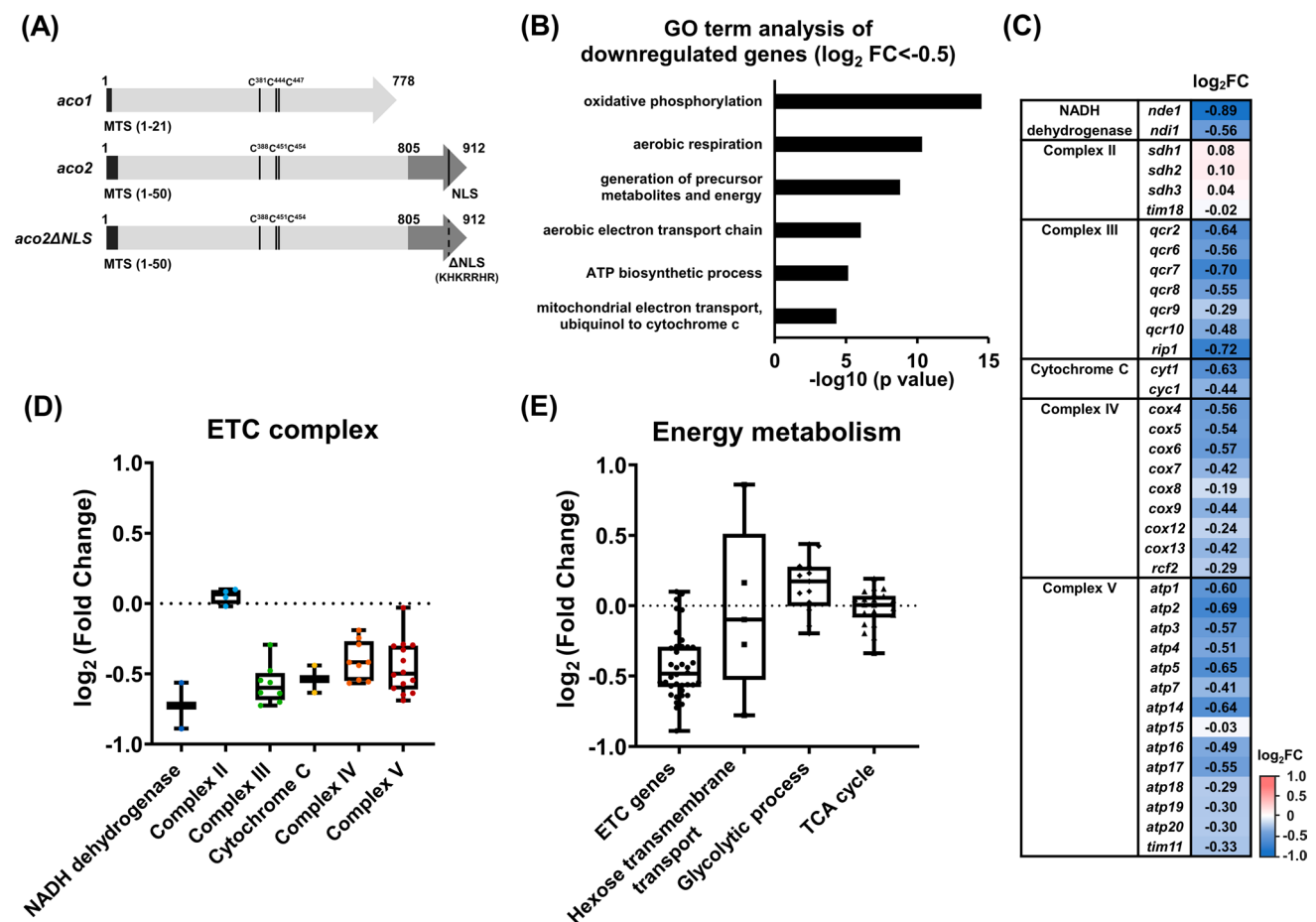


**Fig. 1** Effect of nuclear Aco2 on the mRNA expression of ETC genes. **A** A schematic diagram of genes for the wild-type *aco1*, *aco2* and the *aco2ΔNLS* mutant in *S. pombe* strains. The NLS (nuclear localization signal) sequence (KHKRRHRH) was eliminated in the *aco2ΔNLS* mutant. **B** GO enrichment analysis of downregulated genes ($\log_2$FC < -0.5, 161 genes). **C** The changes in ETC gene expression are displayed with the value of fold-change ($\log_2$FC) and indicated colors. **D** and **E** Box plot illustrating the expressional changes in (**D**) ETC genes categorized by complexes and (**E**) genetic classification of the energy metabolism, comparing the *aco2ΔNLS* mutant with the wild-type strain

Gene Ontology (GO) terms in the biological process of the 161 downregulated genes. The annotated genes are listed in Table S3. This analysis showed that GO categories related to mitochondrial electron transport chain (ETC) and oxidative phosphorylation were significantly enriched ($p < 0.01$) among the genes downregulated in the *aco2ΔNLS* mutant (Fig. 1B). Using information from the biological process annotation of oxidative phosphorylation (GO:0006119) within the *S. pombe* genome database (Pombase), we organized the genes associated with each ETC complex into groups. When we compared the gene expression levels of each complex in the wild-type and *aco2ΔNLS* mutant, we observed that all genes within the ETC complexes, except those in complex II, exhibited significant downregulation (Fig. 1C and D). It was known that genes involved in the ETC, TCA cycle, and hexose transporters undergo upregulation, while genes in glycolysis pathway are downregulated in non-fermentable carbon source (Malecki et al., 2016). Therefore, we investigated the pattern of expression across these biological categories. Interestingly, the *aco2ΔNLS* mutant exhibited expression changes only in ETC gene category and not in other categories [hexose transmembrane transport (GO:0008645), glycolytic process (GO:0061621),

and tricarboxylic acid cycle (GO:0006099)], suggesting that the reduction in ETC genes expression observed in the mutant was not a result of shifts in cellular respiratory conditions (Fig. 1E).

## Reduced mRNA and Protein Expression of Nuclear-Encoded ETC Genes in Mutant

qRT-PCR analysis validated that the expression of *ndi1*, *qcr2*, *cox13*, and *atp2* genes, associated with ETC complexes, respectively, was decreased in the *aco2ΔNLS* mutant (Fig. 2A). Consistent with the RNA-seq results, the expression levels of *sdh1* and *sdh2* genes from complex II showed no difference between the wild-type and the mutant (Fig. 2B). It is noteworthy that genes encoded in the mitochondrial genome, such as *cox1*, *cox2*, and *cox3*, were not altered in the *aco2ΔNLS* mutant (Fig. 2C). In other words, only the gene expression of nuclear-encoded ETC components is affected by the absence of Aco2 in the nucleus. Additionally, we confirmed through western blot analysis that the expression of 5FLAG-tagged Qcr2 and Cox13 proteins was reduced in the *aco2ΔNLS* mutant (Fig. 2D). Taken together, nuclear Aco2 appears to be essential for the
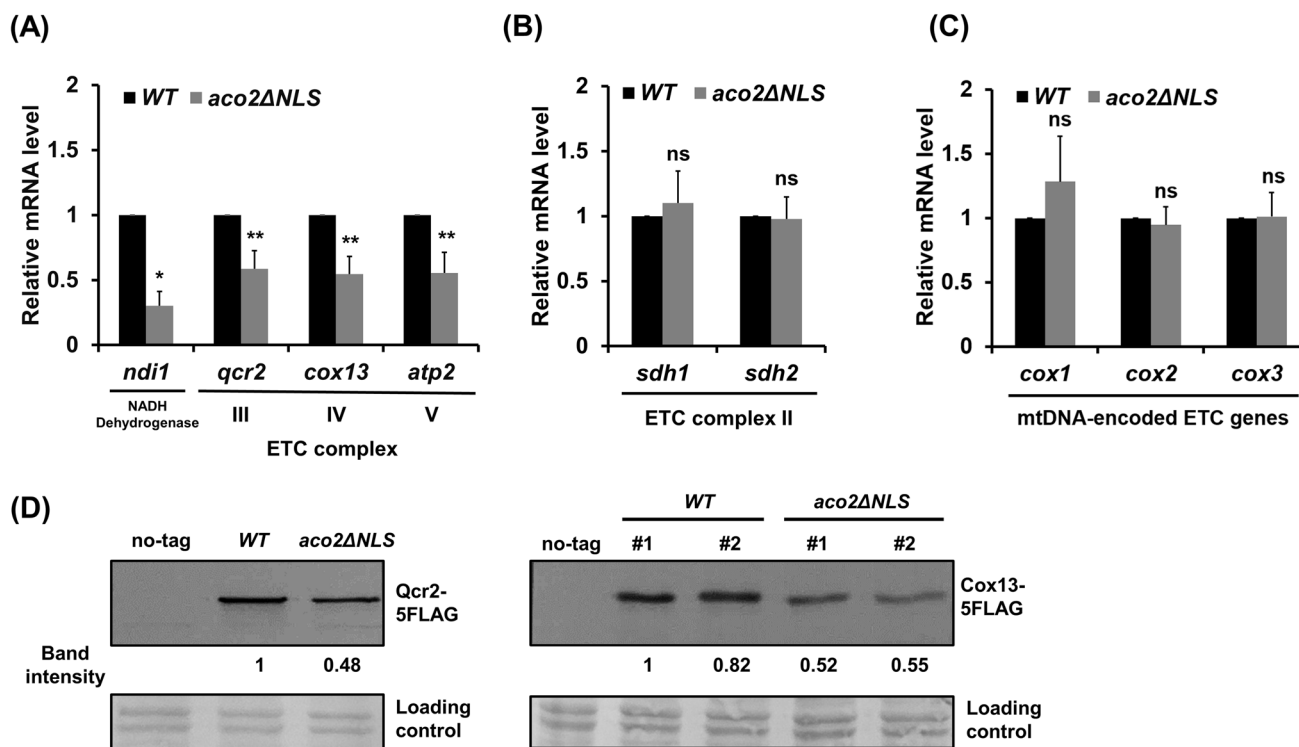


**Fig. 2** Validation of decrease in the expression of nuclear-encoded ETC genes. **A–C** Relative mRNA levels of genes encoding ETC genes in the nucleus and mitochondria. The relative expression of (**A**) nuclear-encoded ETC genes (NADH dehydrogenase, Complex III, IV, and V), (**B**) succinate dehydrogenases (Complex II), and (**C**) mitochondrial-encoded ETC genes were measured in the wild-type (WT) and the *aco2ΔNLS* mutant strains by using qRT-PCR. Data were normalized by *act1* mRNA. **D** Western blot analysis of Qcr2 (Complex III) and Cox13 (Complex IV) of the wild-type (WT) and the *aco2ΔNLS* mutant strains. Ponceau S staining was used as a loading control

expression of the majority of nuclear-encoded ETC genes, except those within complex II.

## Absence of Nuclear Aco2 Leads to Respiratory Growth Defects

To investigate the potential effects of repressed ETC gene activity on the respiratory growth of *S. pombe*, we observed the growth rate of the *aco2ΔNLS* mutant compared to that of the wild-type strain. Cells were cultured in media containing low glucose (0.1% glucose) or alternative carbon sources like galactose and glycerol, which are considered environments supporting respiratory-dependent proliferation (Takeda et al., 2015). In the growth curve analysis, both the wild-type and the *aco2ΔNLS* mutant strains exhibited comparable growth rates in standard minimal media (EMM) containing 2% glucose (Fig. 3A). However, a decrease in the growth rate was noted for the *aco2ΔNLS* mutant strain when grown in the 0.1% glucose media (Fig. 3B). To clarify the respiratory growth impairment of the *aco2ΔNLS* mutant, we performed a spotting assay using non-fermentable carbon sources such as galactose and glycerol. The results demonstrated distinct growth defects in the *aco2ΔNLS* mutant cultivated on media containing 0.1% glucose and non-fermentable carbon sources under aerobic conditions (Fig. 3C). We

also performed a spotting assay under anaerobic conditions and found no noticeable difference in growth rate between the wild-type and mutant (Fig. 3C). These results suggest that the lack of the nuclear Aco2 specifically impacts cellular respiration rather than fermentation processes.

## Catalytic Activity of Aco2 is not Required for the Regulation of ETC Genes

In a recent study, we discovered that the catalytic activity of Aco2 is not essential for facilitating the degradation of iron-transporter mRNAs *in S. pombe* (Cho et al., 2021). We wondered whether nuclear Aco2 might also contribute to controlling the expression of nuclear-encoded ETC genes even without enzymatic activity. To explore this aspect, we conducted a complementation assay using the *aco2ΔNLS* mutant expressing either the wild-type Aco2 (*aco2ΔNLS + aco2*) or non-catalytic Aco2 [*aco2ΔNLS + aco2(3CS)*] (Fig. 4). Non-catalytic Aco2 was generated by substituting serine for three conserved cysteine residues at positions 388, 451, and 454 of Aco2 (Cho et al., 2021). The results of the complementation assay revealed that the substitution mutation displayed effects comparable to those of wild-type Aco2. The respiratory growth defect in the *aco2ΔNLS* mutant was rescued by the expression of either the wild-type Aco2 or the non-catalytic
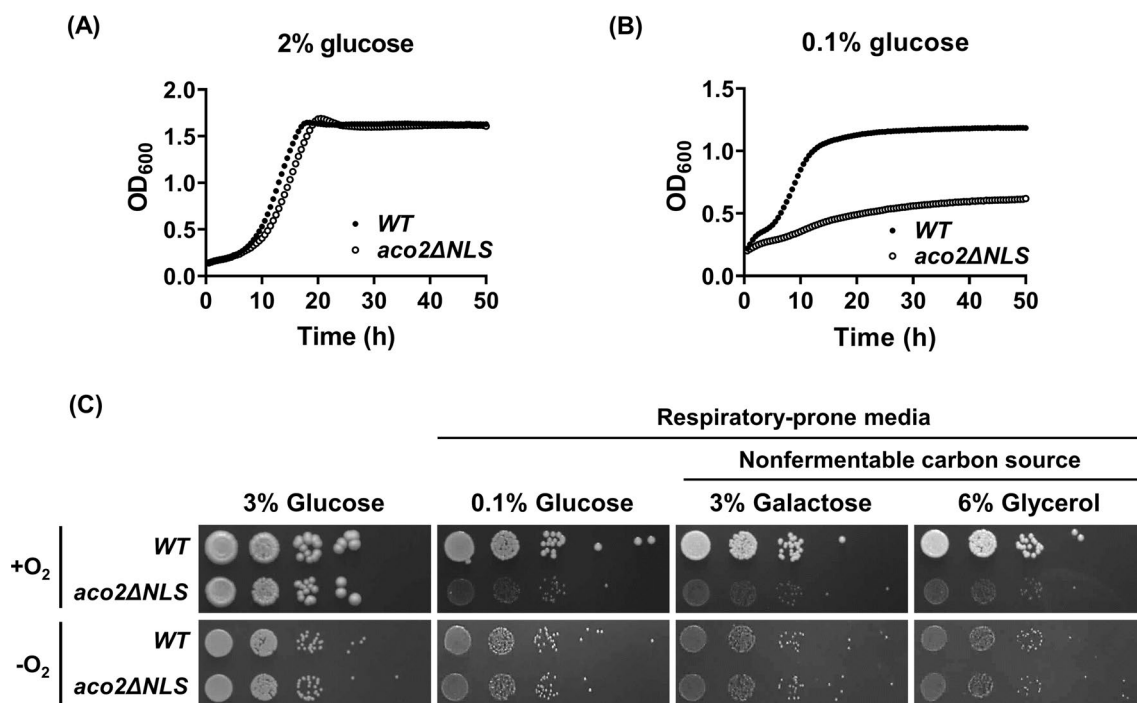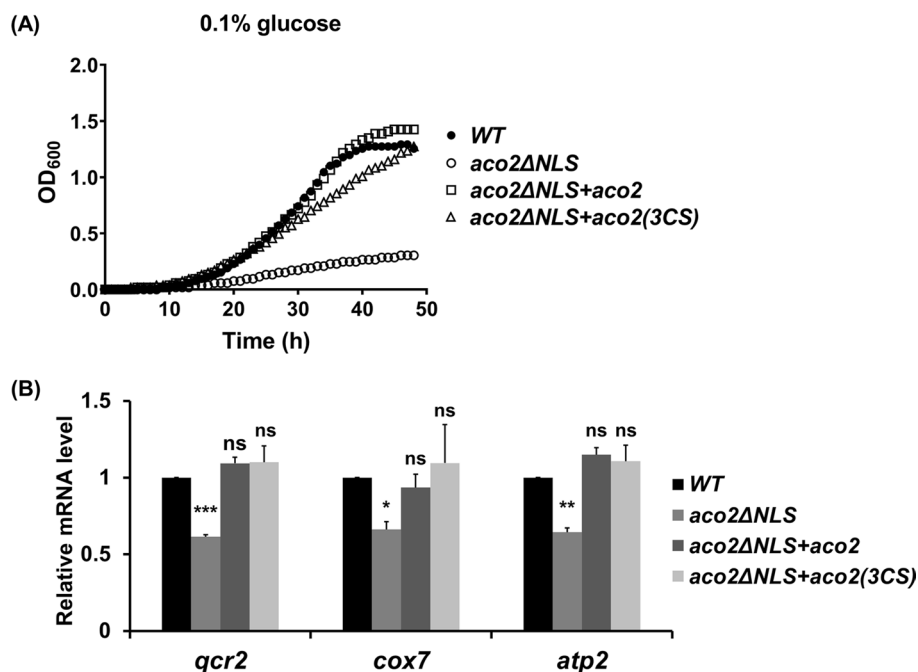


**Fig. 3** Growth deficiency of the *aco2ΔNLS* mutant strain in respiratory-prone media. **A** and **B** Growth curve analysis of the wild-type and the *aco2ΔNLS* in (**A**) 2% glucose and (**B**) 0.1% glucose EMM media. **C** Spotting assay of the wild-type (WT) and the *aco2ΔNLS* mutant strains on YE media with respiratory-prone carbon sources, including 0.1% glucose, 3% galactose + 0.1% glucose, or 6% glycerol + 0.1% glucose. The plates were incubated at 32°C under aerobic or anaerobic conditions

Aco2 (Fig. 4A). Additionally, the decreased expression level of ETC genes in the mutant was also recovered (Fig. 4B). These findings demonstrate that the catalytic activity of Aco2 is irrelevant to its influence on the expression of ETC genes.

## mRNA Stability of ETC Genes was not Changed in the *aco2ΔNLS* Mutant

Considering the role of nuclear/cytosolic Aco2 in the degradation of mRNA associated with iron-uptake genes in fission yeast (Cho et al., 2021), Aco2 could also affect the degradation of ETC genes, leading to the downregulation

of a majority of ETC genes in the *aco2ΔNLS* mutant. To test our hypothesis, we compared the mRNA stability of representative ETC genes from complex III (*qcr2*), complex IV (*cox13*), and complex V (*atp2*) between the wild-type and *aco2ΔNLS* mutant (Fig. 5). Unexpectedly, there were no differences in the decay rates of *qcr2*, *cox13*, and *atp2* mRNAs. Instead, the amount of ETC mRNAs in the *aco2ΔNLS* mutant was lower than that in the wild-type from the beginning, as shown in Fig. 2 (Fig. 5). These findings suggest that nuclear Aco2 is likely involved in regulating ETC gene expression at the transcriptional level rather than the post-translational level.
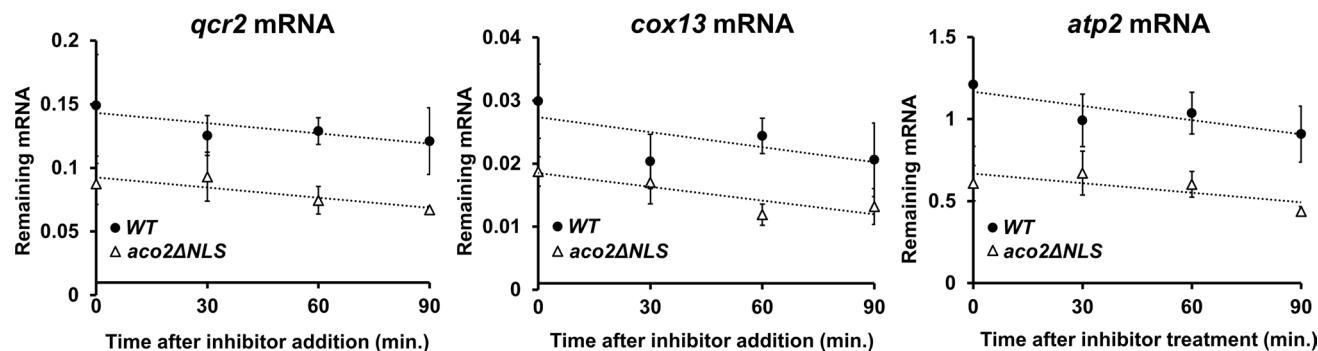


**Fig. 5** The mRNA decay analysis of ETC genes in the wild-type and *aco2ΔNLS* mutant strains mRNA decay profiles of the wild-type and *aco2ΔNLS* strains. Cells were treated with 1,10-phenanthroline (300 µg/ml) as a transcriptional inhibitor and harvested at each time point for RNA analysis. Graph symbols of the wild-type (black circle) and *aco2ΔNLS* (white triangle) represent three independent experiments average values ± SEM

## Interplay Between the Php Complex and Nuclear Aco2 in the Regulation of ETC Genes

Given that the overall expression of nuclear-encoded ETC genes was decreased in the *aco2ΔNLS* mutant, Aco2 might interact with transcription factors associated with ETC genes. While global regulators of the ETC complex in *S. pombe* remain unidentified, the Php complex was expected to regulate genes related to respiration, the TCA cycle, and the iron response (Mercier et al., 2008). The *php2* deletion

mutant showed the respiratory growth defect and downregulation of the *cyc1* and *rip1* genes (Takuma et al., 2013). Therefore, we examined the transcriptional levels of Php complex subunits (Php2, Php3, Php4, and Php5) in both wild-type and mutant strains, but transcriptional change was not observed (Fig. 6A). Subsequently, we investigated the expression of ETC genes in the *php3Δ*, *php5Δ*, and *aco2ΔNLS* mutants using qRT-PCR. The expression level of ETC genes, except for those belonging to complex II, showed a significant reduction in *php3Δ* and *php5Δ*
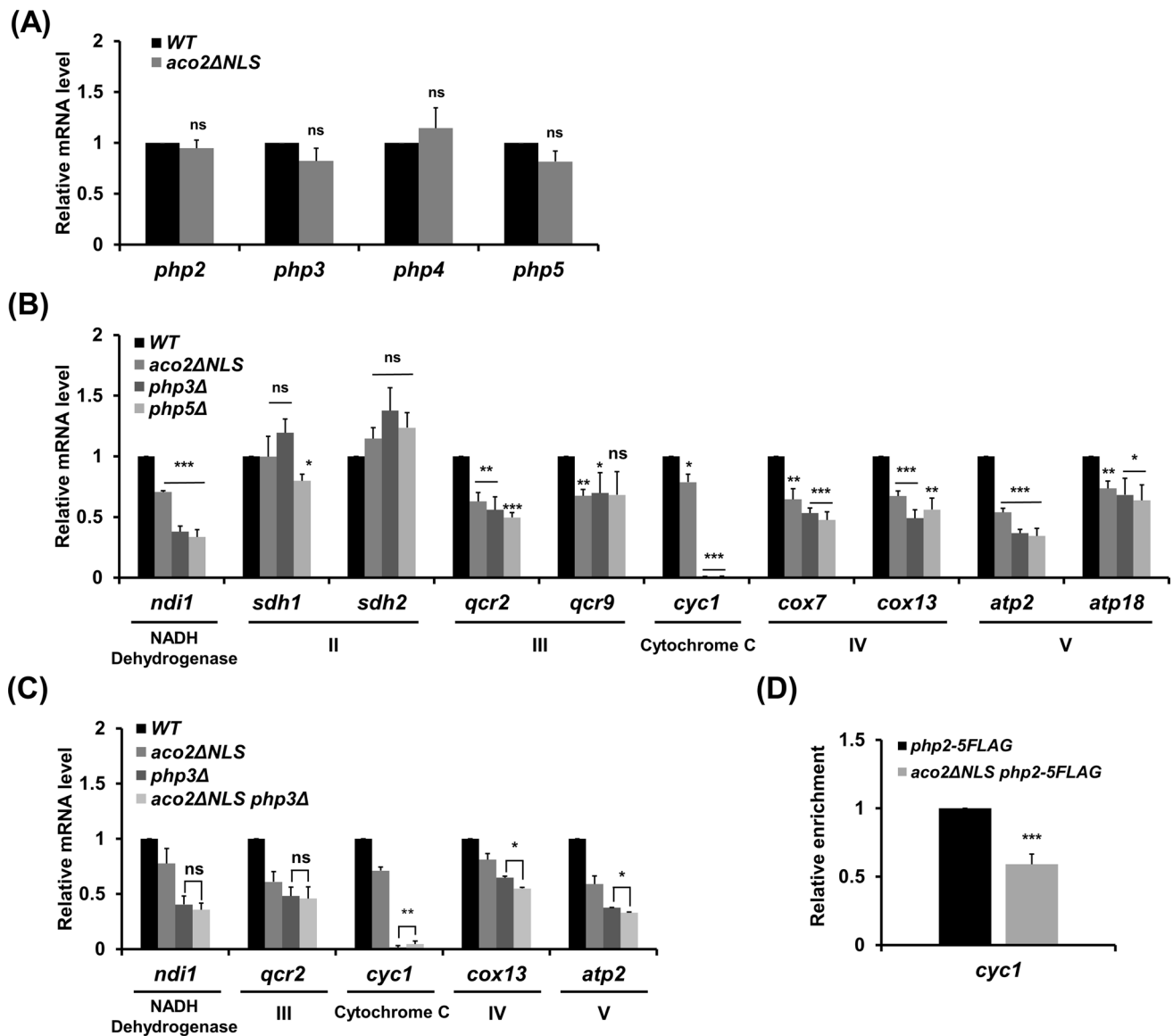


**Fig. 6** Genetic interaction between the Php complex and nuclear Aco2 in the regulation of ETC genes. **A** The relative mRNA levels of Php complex in the wild-type (WT) and *aco2ΔNLS* mutant. **B** The relative mRNA levels of ETC genes including NADH dehydrogenase, ETC complex II, III, cytochrome C, complex IV, and V in the WT strain, *aco2ΔNLS*, *php3Δ*, and *php5Δ* mutants. **C** The relative

mRNA levels of ETC genes in the WT strain, *aco2ΔNLS*, *php3Δ*, and *aco2ΔNLS php3Δ* mutants. Data were normalized by *act1* mRNA. **D** Relative enrichment for the *cyc1* upstream region using chromatin immunoprecipitation (ChIP) assay in the *php2-5FLAG* and *aco2ΔNLS php2-5FLAG* strain. Data were normalized by the *act1* gene and input control

mutants, similar to the *aco2ΔNLS* mutant (Fig. 6B). To identify genetic interaction between the Php complex and nuclear Aco2, we mated two mutant strains, the *php3Δ* and *aco2ΔNLS* mutant. Interestingly, the double mutant strain exhibited a similar downregulation of ETC genes like that seen in the *php3Δ* mutant (Fig. 6C). To elucidate the correlation between the Php complex and nuclear Aco2 in the transcriptional regulation of ETC genes, we conducted a chromatin immunoprecipitation (ChIP) assay using 5FLAG-tagged Php2, one of the DNA-binding subunits of the Php complex. We observed a decrease in the binding affinity of the Php2 protein in the *cyc1* promoter region in the absence of nuclear Aco2 (Fig. 6D). Based on these findings, we suggest that the Php complex and nuclear Aco2 may serve as potential regulators of nuclear-encoded ETC genes within the same regulatory pathway.

## Discussion

*S. pombe* Aco2 has a distinctive domain arrangement consisting of an N-terminal aconitase domain with MTS and a C-terminal mitochondrial ribosomal domain with NLS (Jung et al., 2015). Our previous studies showed that Aco2 is required for mitochondrial translation (Jung et al., 2015) and heterochromatin maintenance in the nucleus along with the heterochromatin protein Chp1 (Jung et al., 2019). To further comprehensively investigate the role of Aco2 in the nucleus, we conducted RNA-seq analyses and observed that iron-uptake genes are upregulated in the *aco2ΔNLS* mutant strain (Cho et al., 2021). We found that iron-uptake genes are post-transcriptionally regulated by both nuclear and cytosolic Aco2 (Cho et al., 2021). Additionally, we observed that ETC genes are downregulated in the *aco2ΔNLS* mutant strain (Figs. 1 and 2), but the mechanism of the downregulation has not been established.

Mitochondrial defects can communicate with the nucleus via mitochondrial retrograde signaling (Liu & Butow, 2006). To distinguish Aco2's role in the nucleus from thoes in mitochondria, we investigated aconitase's catalytic residue and mitochondrial translation. First, we discovered that a substitution mutation affecting three conserved cysteine residues (388, 451, and 454) in Aco2 could restore both growth impairment and expression of ETC genes in the *aco2ΔNLS* mutant strain (Fig. 4). This suggests that the regulation of ETC genes is not dependent on Aco2's catalytic function. Second, our previous research showed that mitochondrially targeted Aco2 ribosomal domain (MTS-Aco2ΔNLS) plays a role in mitochondrial translation (Jung et al., 2015). Therefore, it is unlikely that potential mitochondrial dysfunction in the *aco2ΔNLS* mutant account for the downregulation of ETC genes.

Transcriptional regulation of ETC genes has been studied in yeasts and higher eukaryotes. In *S. cerevisiae*, the CCAAT box has been reported to be present within promoters of genes associated with respiratory functions (McNabb et al., 1997). The Hap complex was identified for its capacity to bind to the CCAAT box located upstream of the activation sequence (UAS) element of CYC1, which encodes iso-1-cytochrome C (Forsburg & Guarente, 1989; Olesen et al., 1987), and other cytochrome genes, functioning as a central regulator of respiratory metabolism (Buschlen et al., 2003; Schüller, 2003). Homologs of the Hap complex components are also present in other yeasts, such as *Candida albicans* (Baek et al., 2008; Johnson et al., 2005; Singh et al., 2011), *Candida glabrata* (Thiebaut et al., 2017; Ueno et al., 2011), *Aspergillus fumigatus* (Gsaller et al., 2014; Thiebaut et al., 2017), *Cryptococcus neoformans* (Jung et al., 2010), and *S. pombe* (McNabb et al., 1997; Olesen et al., 1991). In *S. pombe*, Php2/3/5 serve as transcriptional activators, while Php4 counteracts the activation role of Php2/3/5 (Mercier et al., 2008). Deletion of *php2* showed low respiratory activity, and downregulation of *cyc1* and *rip1* genes (Takuma et al., 2013). From these existing understanding, we investigated how the Aco2 triggers the activation of ETC genes in the nucleus together with Php complex, a putative transcriptional regulator of ETC in *S. pombe*.

Since the expression of ETC genes overall was repressed in the *aco2ΔNLS* mutant, we examined the functional interaction between Aco2 and the Php complex. We observed the downregulation of overall ETC genes in *php3Δ* and *php5Δ* mutants, similar to the *aco2ΔNLS* mutant strain (Fig. 6B). Subsequently, the double mutant strain with both *php3Δ* and *aco2ΔNLS* mutations exhibited a similar downregulation of ETC genes as observed in the single mutant strains (Fig. 6C). Given that Php complex are well known as CCAAT motif binding factor, we performed ChIP assay targeting the CCAAT motif within the upstream region of cytochrome C (*cyc1*), well known as target gene of Php complex (Mercier et al., 2008). the *aco2ΔNLS* mutant strain, the binding affinity of the Php2 protein was reduced by approximately half. Together, these finding suggests that nuclear Aco2 operates within the same pathway as the Php complex, affecting Php binding and thereby regulating nuclear-encoded ETC genes. Although we propose a functional connection between nuclear Aco2 and the Php complex, further genetic and biochemical investigations are required to better understand the underlying mechanism.

## Declarations

## References

Alén, C., & Sonenshein, A. L. (1999). *Bacillus subtilis* aconitase is an RNA-binding protein. *Proceedings of the National Academy of Sciences of the United States of America, 96*, 10412–10417.

Baek, Y. U., Li, M., & Davis, D. A. (2008). *Candida albicans* ferric reductases are differentially regulated in response to distinct forms of iron limitation by the Rim101 and CBF transcription factors. *Eukaryotic Cell, 7*, 1168–1179.

Banerjee, S., Nandyala, A. K., Raviprasad, P., Ahmed, N., & Hasnain, S. E. (2007). Iron-dependent RNA-binding activity of *Mycobacterium tuberculosis* aconitase. *Journal of Bacteriology, 189*, 4046–4052.

Beinert, H., Kennedy, M. C., & Stout, C. D. (1996). Aconitase as iron-minus signSulfur Protein, Enzyme, and Iron-Regulatory Protein. *Chemical Reviews, 96*, 2335–2374.

Benjamin, J. A., & Massé, E. (2014). The iron-sensing aconitase B binds its own mRNA to prevent sRNA-induced mRNA cleavage. *Nucleic Acids Research, 42*, 10023–10036.

Bolger, A. M., Lohse, M., & Usadel, B. (2014). Trimmomatic: A flexible trimmer for Illumina sequence data. *Bioinformatics, 30*, 2114–2120.

Boukouris, A. E., Zervopoulos, S. D., & Michelakis, E. D. (2016). Metabolic enzymes moonlighting in the nucleus: Metabolic regulation of gene transcription. *Trends in Biochemical Sciences, 41*, 712–730.

Buschlen, S., Amillet, J. M., Guiard, B., Fournier, A., Marcireau, C., & Bolotin-Fukuhara, M. (2003). The *S. cerevisiae* HAP complex, a key regulator of mitochondrial function, coordinates nuclear and mitochondrial gene expression. *Comparative and Functional Genomics, 4*, 37–46.

Castello, A., Hentze, M. W., & Preiss, T. (2015). Metabolic enzymes enjoying new partnerships as RNA-binding proteins. *Trends in Endocrinology and Metabolism, 26*, 746–757.

Cho, S. Y., Jung, S. J., Kim, K. D., & Roe, J. H. (2021). Non-mitochondrial aconitase regulates the expression of iron-uptake genes by controlling the RNA turnover process in fission yeast. *Journal of Microbiology, 59*, 1075–1082.

Dupuy, J., Volbeda, A., Carpentier, P., Darnault, C., Moulis, J. M., & Fontecilla-Camps, J. C. (2006). Crystal structure of human iron regulatory protein 1 as cytosolic aconitase. *Structure, 14*, 129–139.

Forsburg, S. L., & Guarente, L. (1989). Identification and characterization of HAP4: A third component of the CCAAT-bound HAP2/HAP3 heteromer. *Genes & Development, 3*, 1166–1178.

Forsburg, S. L., & Rhind, N. (2006). Basic methods for fission yeast. *Yeast, 23*, 173–183.

Gourley, B. L., Parker, S. B., Jones, B. J., Zumbrennen, K. B., & Leibold, E. A. (2003). Cytosolic aconitase and ferritin are regulated by iron in *Caenorhabditis elegans*. *Journal of Biological Chemistry, 278*, 3227–3234.

Gray, N. K., Pantopoulos, K., Dandekar, T., Ackrell, B. A., & Hentze, M. W. (1996). Translational regulation of mammalian and *Drosophila* citric acid cycle enzymes via iron-responsive elements. *Proceedings of the National Academy of Sciences of the United States of America, 93*, 4925–4930.

Gsaller, F., Hortschansky, P., Beattie, S. R., Klammer, V., Tuppatsch, K., Lechner, B. E., Rietzschel, N., Werner, E. R., Vogan, A. A., Chung, D., et al. (2014). The Janus transcription factor HapX controls fungal adaptation to both iron starvation and iron excess. *The EMBO Journal, 33*, 2261–2276.

Jeffery, C. J. (2015). Why study moonlighting proteins? *Frontiers in Genetics, 6*, 211.

Jeffery, C. J. (2020). Enzymes, pseudoenzymes, and moonlighting proteins: Diversity of function in protein superfamilies. *The FEBS Journal, 287*, 4141–4149.

Johnson, D. C., Cano, K. E., Kroger, E. C., & McNabb, D. S. (2005). Novel regulatory function for the CCAAT-binding factor in *Candida albicans*. *Eukaryotic Cell, 4*, 1662–1676.

Jung, S. J., Choi, Y., Lee, D., & Roe, J. H. (2019). Nuclear aconitase antagonizes heterochromatic silencing by interfering with Chp1 binding to DNA. *Biochemical and Biophysical Research Communications, 516*, 806–811.

Jung, S. J., Seo, Y., Lee, K. C., Lee, D., & Roe, J. H. (2015). Essential function of Aco2, a fusion protein of aconitase and mitochondrial ribosomal protein bL21, in mitochondrial translation in fission yeast. *FEBS Letters, 589*, 822–828.

Jung, W. H., Saikia, S., Hu, G., Wang, J., Fung, C. K., D'Souza, C., White, R., & Kronstad, J. W. (2010). HapX positively and negatively regulates the transcriptional response to iron deprivation in *Cryptococcus neoformans*. *PLoS Pathogens, 6*, e1001209.

Kim, D., Paggi, J. M., Park, C., Bennett, C., & Salzberg, S. L. (2019). Graph-based genome alignment and genotyping with HISAT2 and HISAT-genotype. *Nature Biotechnology, 37*, 907–915.

Kim, E. J., Cho, Y. J., Chung, W. H., & Roe, J. H. (2020). The role of Rsv1 in the transcriptional regulation of genes involved in sugar metabolism for long-term survival. *The FEBS Journal, 287*, 878–896.

Klausner, R. D., & Rouault, T. A. (1993). A double life: Cytosolic aconitase as a regulatory RNA binding protein. *Molecular Biology of the Cell, 4*, 1–5.

Liao, Y., Smyth, G. K., & Shi, W. (2014). featureCounts: An efficient general purpose program for assigning sequence reads to genomic features. *Bioinformatics, 30*, 923–930.

Lind, M. I., Missirlis, F., Melefors, O., Uhrigshardt, H., Kirby, K., Phillips, J. P., Söderhäll, K., & Rouault, T. A. (2006). Of two cytosolic aconitases expressed in *Drosophila*, only one functions as an iron-regulatory protein. *The Journal of Biological Chemistry, 281*, 18707–18714.

Liu, Z., & Butow, R. A. (2006). Mitochondrial retrograde signaling. *Annual Review of Genetics, 40*, 159–185.

Love, M. I., Huber, W., & Anders, S. (2014). Moderated estimation of fold change and dispersion for RNA-seq data with DESeq2. *Genome Biology, 15*, 550.

Lushchak, O. V., Piroddi, M., Galli, F., & Lushchak, V. I. (2014). Aconitase post-translational modification as a key in linkage between Krebs cycle, iron homeostasis, redox signaling, and metabolism of reactive oxygen species. *Redox Report, 19*, 8–15.

Malecki, M., Bitton, D. A., Rodríguez-López, M., Rallis, C., Calavia, N. G., Smith, G. C., & Bähler, J. (2016). Functional and regulatory profiling of energy metabolism in fission yeast. *Genome Biology, 17*, 240.

McNabb, D. S., Tseng, K. A., & Guarente, L. (1997). The *Saccharomyces cerevisiae* Hap5p homolog from fission yeast reveals two conserved domains that are essential for assembly of heterotetrameric CCAAT-binding factor. *Molecular and Cellular Biology, 17*, 7008–7018.

Mercier, A., Watt, S., Bähler, J., & Labbé, S. (2008). Key function for the CCAAT-binding factor Php4 to regulate gene expression in response to iron deficiency in fission yeast. *Eukaryotic Cell, 7*, 493–508.

Muckenthaler, M. U., Galy, B., & Hentze, M. W. (2008). Systemic iron homeostasis and the iron-responsive element/iron-regulatory protein (IRE/IRP) regulatory network. *Annual Review of Nutrition, 28*, 197–213.

Olesen, J. T., Fikes, J. D., & Guarente, L. (1991). The *Schizosaccharomyces pombe* homolog of *Saccharomyces cerevisiae* HAP2 reveals selective and stringent conservation of the small essential core protein domain. *Molecular and Cellular Biology, 11*, 611–619.

Olesen, J., Hahn, S., & Guarente, L. (1987). Yeast HAP2 and HAP3 activators both bind to the CYC1 upstream activation site, UAS2, in an interdependent manner. *Cell, 51*, 953–961.

Piccinelli, P., & Samuelsson, T. (2007). Evolution of the iron-responsive element. *RNA, 13*, 952–966.

Rouault, T. A. (2006). The role of iron regulatory proteins in mammalian iron homeostasis and disease. *Nature Chemical Biology, 2*, 406–414.

Schüller, H. J. (2003). Transcriptional control of nonfermentative metabolism in the yeast *Saccharomyces cerevisiae*. *Current Genetics, 43*, 139–160.

Singh, R. P., Prasad, H. K., Sinha, I., Agarwal, N., & Natarajan, K. (2011). Cap2-HAP complex is a critical transcriptional regulator that has dual but contrasting roles in regulation of iron homeostasis in *Candida albicans*. *Journal of Biological Chemistry, 286*, 25154–25170.

Takeda, K., Starzynski, C., Mori, A., & Yanagida, M. (2015). The critical glucose concentration for respiration-independent proliferation of fission yeast, *Schizosaccharomyces pombe*. *Mitochondrion, 22*, 91–95.

Takuma, K., Ohtsuka, H., Azuma, K., Murakami, H., & Aiba, H. (2013). The fission yeast *php2* mutant displays a lengthened chronological lifespan. *Bioscience, Biotechnology, and Biochemistry, 77*, 1548–1555.

Thiebaut, A., Delaveau, T., Benchouaia, M., Boeri, J., Garcia, M., Lelandais, G., & Devaux, F. (2017). The CCAAT-binding complex controls respiratory gene expression and iron homeostasis in *Candida glabrata*. *Scientific Reports, 7*, 3531.

Ueno, K., Matsumoto, Y., Uno, J., Sasamoto, K., Sekimizu, K., Kinjo, Y., & Chibana, H. (2011). Intestinal resident yeast *Candida glabrata* requires Cyb2p-mediated lactate assimilation to adapt in mouse intestine. *PLoS ONE, 6*, e24759.

Volz, K. (2008). The functional duality of iron regulatory protein 1. *Current Opinion in Structural Biology, 18*, 106–111.